

THE PENNSYLVANIA STATE UNIVERSITY
MILLENNIUM SCHOLARS PROGRAM

DEPARTMENT OF MECHANICAL ENGINEERING

Biomechanics of Comb Jellies Swimming in Turbulent Flow

CARLOS ABARCA

SPRING 2021

A thesis
submitted in partial fulfillment
of the requirements
for a baccalaureate degree
in Mechanical Engineering

Reviewed and approved* by the following:

Dr. Margaret Byron

Assistant Professor of Mechanical Engineering

Thesis Advisor

Dr. Bo Cheng

Associate Professor of Mechanical Engineering

Second Reader

*Signatures are on file in the Millennium Scholars Program Office

Abstract

Ctenophores are the largest animals on Earth that use cilia as their primary swimming mechanism. These animals possess useful swimming abilities, such as high maneuverability. We are interested in exploring the advantages of primarily swimming with cilia at larger Reynolds numbers. We used two flow tanks to investigate how ctenophores altered their swimming behavior in response to fluid motion. The first tank was a water flume designed to allow observation of the motion of the animals' cilia in varying mean flow speeds. The second tank created turbulent flow using underwater speakers, with no background current; we tracked the motion of freely-swimming ctenophores in different levels of turbulence to find potential differences in overall swimming behavior. We found that the animals tended to increase their excursion durations as turbulence increased, and that the path of their swimming excursions tended to be less vertical as turbulence increased.

Table of Contents

Abstract.....	i
Table of Contents.....	ii
List of Figures.....	iv
List of Tables.....	v
Acknowledgments.....	vi
Introduction.....	1
Ctenophores.....	1
Water Flume.....	3
Turbulence Tracking.....	4
Literature Review.....	5
Cilia background and Kinematics.....	6
Particle Image Velocimetry.....	8
Project Goals.....	9
Materials and Methods.....	10
Water Flume.....	10
Facility Construction.....	10
Preliminary Flow Data.....	11
Turbulence Tracking.....	13
Turbulence Tank.....	13
Video Tracking.....	14
Expansion and Analysis.....	14
Results.....	16

Excursion Duration	16
Velocity	17
Directionality	18
Distribution	20
Discussion and Conclusions	22
Appendix A	26
Appendix B	27
Appendix C	31
Works Cited	38

List of Figures

Figure 1. Cilia Kinematics.....	1
Figure 2. Cydippid Ctenophore.....	2
Figure 3. Ctenophore Biodiversity.....	6
Figure 4. Water Flume.....	11
Figure 5. Gripper Design	11
Figure 6. Calibration.....	12
Figure 7. Water Flume PIV	13
Figure 8. Turbulence tank	14
Figure 9. Tracked Ctenophore Positions	15
Figure 10. Excursion duration plots (data from table C-1).....	17
Figure 11. Plots for average and maximum speeds (data from table C-2).....	18
Figure 12. Net Displacement.....	19
Figure 13. Verticality.....	19
Figure 14. Tortuosity plots (data from table C-5).....	20
Figure 15. Excursion Distribution.....	21

List of Tables

Table 1. Null and Alternative Hypotheses for the water flume project.....	3
Table 2. Null and Alternative Hypotheses for the turbulence tracking project.....	4
Table C-1. Excursion durations (seconds).....	31
Table C-2. Average and maximum speeds (centimeters/second).....	32
Table C-3. Net horizontal and vertical displacement (centimeters).....	33
Table C-4. Verticality (nondimensional).....	35
Table C-5. Tortuosity (nondimensional)	36

Acknowledgements

I want to express my gratitude for Dr. Margaret Byron. She has been patient, supportive, and understanding during my time as an undergraduate researcher. She has always put her faith into me and I am thankful for her guidance through this journey.

I want to thank everyone in the Millennium Scholars Program. From the advisors to the students, they have built a network and family for me to count on and be supported by.

I would like to thank my family. They have helped me through difficult times through journeys of undergraduate research and studies and I am very appreciative of their never-ending support.

Introduction

Ctenophores

Ctenophores (comb jellies) are a type of predatory marine zooplankton. Their prey mainly consists of smaller zooplankton and other ctenophores. Their bodies mainly consist of a gelatinous material called mesoglea, along with muscle tissue [1]. Ctenophores are the largest animals in the world who rely primarily on cilia to swim. Their cilia are grouped into millimeter-long “comb plates”, which are the largest known ciliary structure [2]. These comb plates (also called “ctenes”) are composed of thousands of cilia, which are bundled together and move as a unit. Figure 1 shows the motion the cilia make when swimming.

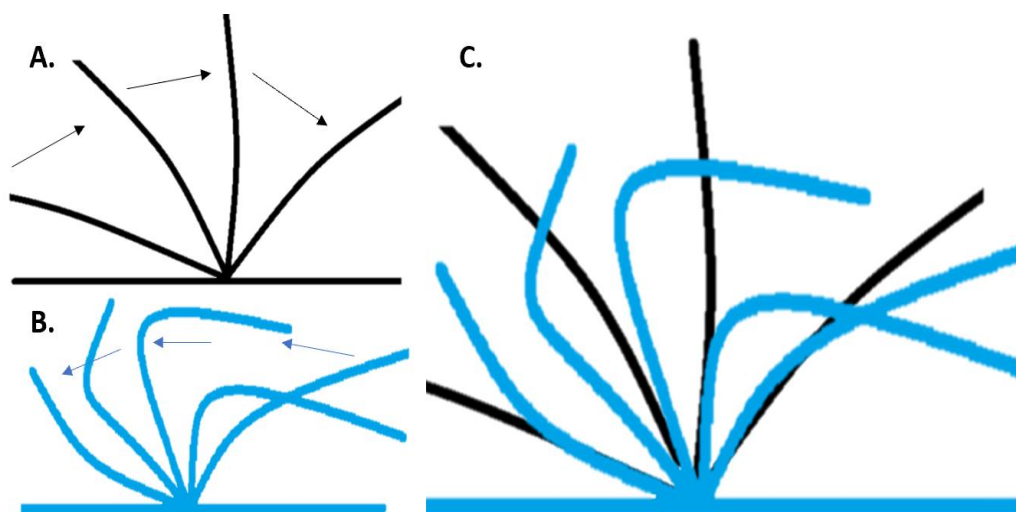


Figure 1. Cilia kinematics. [A] shows the power stroke motion of the cilia. [B] shows the recovery stroke motion of the cilia. [C] shows a complete beat cycle.

Each animal has eight rows of these comb plates, which are evenly spaced around their bodies. In figure 2, the full morphology of a ctenophore is shown, specifically how the ctene rows of the animal longitudinally circumscribe its body. At this relatively large scale (centimeters), swimming with the primary use of cilia is limited to ctenophores alone. It is still

unclear how the swimming mechanics of cilia work at the larger scales of ctenophores, compared to the more typical scales found in microorganisms, such as *Paramecium*, which is about 251 μm long with 10-12 μm cilia [3].

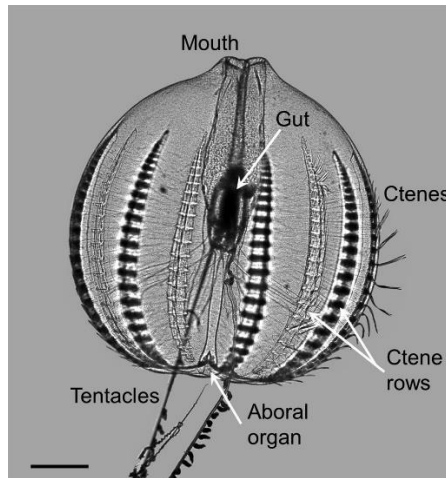


Figure 2. Cydippid ctenophore. Close up of the ctenophore *Pleurobrachia bachei*, showing visible ctenes and ctenes rows. Taken from [4].

When comparing ctenophores to microorganisms, both of which can rely on cilia, it is important to acknowledge that they operate at different Reynolds numbers. The Reynolds number, or Re , is a dimensionless ratio which represents the ratio of inertial to viscous forces in a flow. It is defined as $Re \equiv \frac{\rho UL}{\mu}$, where ρ is the fluid density, U is a representative velocity scale, L is a representative length, and μ is the fluid dynamic viscosity. Organisms that operate at low Reynolds numbers have to develop unique swimming mechanisms because the flow is dominated by viscosity, so there is no ability to glide: when the animal stops moving its appendages, it stops moving through the water. One common low-Reynolds number mechanism is the use of cilia, common in microorganisms and on the tissues of larger organisms. Cilia can operate at extremely low Reynolds numbers. For example, *Paramecium* operates at a Re of 10^{-3} , while a single cilia is at 10^{-4} [3]. Ctenophores operate at much larger Re . These organisms,

depending on species, can range from an Re of 100-6000, while their cilia operate at 30-300 [5]. Since these organisms operate at much greater Reynolds numbers, it is interesting to see how they utilize this unique swimming mechanism. Here, we will explore how ctenophores use cilia to control their swimming behavior.

Water Flume

To increase our understanding of ctenophore swimming kinematics, we conducted two complementary studies. Each possessed different methods and goals, but the same overall aim: to investigate the capabilities of large-scale cilia and their responses to ambient flow. For the first study, we designed and constructed a miniature water flume to serve as a testing facility for the animals, where they could be immersed in a controllable mean flow. We aimed to observe the adjustments of the beating cilia of tethered/constrained animals as we increased and decreased the flow speed. Animals can be suspended in the test section of the water flume, which has transparent sides to facilitate high speed imaging and flow visualization.

With these observations, we can gain insight about the animals' reactions to and capabilities in different flow environments. Our hypotheses are outlined in Table 1.

Table 1. Null and Alternative Hypotheses for the water flume project

Specific Aim	Null and Alternative Hypotheses
1	H0: The animals have no reaction to the changes in flow speed (beat frequency does not change). H1: The animals will increase the beat frequency of their cilia as flow speed increases.

Previous work has shown that an increase in beat frequency corresponded to increased swimming speed in freely swimming (untethered) animals [6]. However, it is unknown whether

the reverse holds true in tethered animals (that is, if increased flow speed relative to the body cues the animal to increase beat frequency). The animal may respond to increased ambient flow by increasing its beat frequency, or display a passive response, not taking action against the change. Using the water flume, we will observe the animals' responses to changes in flow.

Turbulence Tracking

Due to the COVID-19 pandemic, flume experiments were not able to proceed as planned (see Methods section for planned work). Instead, we moved to a new experiment that focused on the animals' full body maneuverability instead of the isolated ctenophore rows. We analyzed previously recorded videos of ctenophores swimming in turbulence, using two-dimensional kinematic tracking to measure the animals' swimming trajectories. In these previous experiments, multiple animals were suspended in a tank with underwater speakers mounted on each side. The vibrations from the speakers created turbulence of variable strength, allowing us to explore whether animals behaved differently when exposed to different levels of turbulence. For each trial, 15 to 20 animals swam freely in the tank; we tracked their locations over a five-minute period, focusing on actively-swimming "excursions" away from the walls and bottom of the tank.

The purpose of these experiments was to understand how animals' swimming behavior might be altered by different levels of turbulence, and how their maneuverability may depend on the ambient flow. Our hypotheses for this project are outlined in Table 2.

Table 2. Null and Alternative Hypotheses for the turbulence tracking project

Specific Aim	Null and Alternative Hypotheses
2	H0: Animals will not change their distribution around the tank, no matter the level of turbulence. H1: Animals begin to cluster more towards

	the top or walls of the tank as the level of turbulence increases.
3	H0: Increasing turbulence has no effect on the directionality or speed of swimming. H1: Pronounced differences in animal swimming patterns, such as directionality and speed, will be observed from no-flow (still) to turbulent conditions.

Previous studies observed that turbulence plays a role in regulating ctenophores' behavior and vertical displacement [7], and is known to affect the swimming behavior of many other marine invertebrates [8]–[12]. Turbulence is an ever-present influence in the marine environment. It is therefore important to understand how turbulence changes ctenophores' swimming patterns.

Literature Review

Ctenophores are the largest animals in the world who rely primarily on cilia to swim [2]. These organisms can be found over most of the oceans in the world. They tend to dwell near surface waters and shores. Although most have limited range, certain specimens (such as *Pleurobrachia pileus*) can be found worldwide [13]. Ctenophores are predators that feed primarily on smaller zooplankton. They do not tend to be active hunters and count on their prey coming in contact with them (ambush predation). Due to a wide diversity in feeding modes, predatory mechanics can vary from species to species [2]. These animals can come in all shapes and sizes, shown in Figure 5. Despite this variety, these zooplankton swim primarily with cilia which makes them unique at these Reynolds numbers.

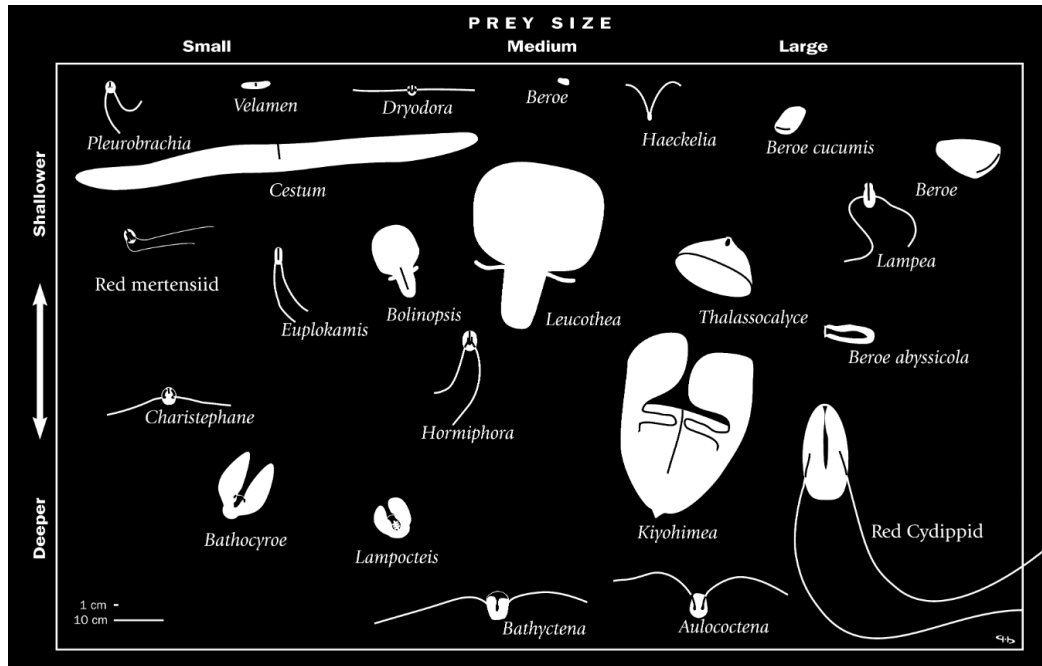


Figure 3. Ctenophore biodiversity. Shows variety of ctenophore shapes and sizes. It also organizes them in depth of habitation and size of their prey. Taken from [14].

Cilia Background and Kinematics

The movement of ctene rows has been a subject of interest since at least 1905, when Parker studied the coordination of the rows in a variety of ctenophore species [15]. Others have focused on the mechanical properties of cilia and the mechanical and neural drivers of their motion [16], [17]. Tamm explored the mechanisms underlying the coordination of the “metachronal wave” which emerges as adjacent ctenes beat in sequence, and concluded that the coupling was primarily hydrodynamic in nature [17], [18]. Further research describes the types of motion the cilia of various organisms can perform. Regarding ctenophores, Blake discusses *Pleurobrachia* and how their comb plates have a metachronal coordination to their beating [19]. This coordination can be affected by different factors. Barlow and Sleight [20] were able to control the beat frequency of the comb plates using electronic signals. They sought to understand if factors like beat frequency or temperature had an effect on the overall coordination of the cilia.

Research began to investigate other factors that affected the swimming capabilities of ctenophores and their cilia. Matsumoto wanted to understand the correlation between ciliary propulsion and body length and ctene length [5]. Studying various species of ctenophores, they were able to calculate the Re , beat frequency and speed for different body and ctene lengths. However due to morphological differences, it was difficult to develop a ctene plate mathematical model. Varying morphologies can lead to variations in swimming kinematics. One study discussed that as the animal got larger, the morphology of the body changed [6]. It was noted that kinematic adjustment from the animals could overcome morphological limitations.

Ctenophores are capable of swimming due to the propulsive forces created by their cilia. The mechanics of micron-scale cilia are well-studied [21], but millimeter-scale cilia (found in ctenophores) are less well-studied, though scattered studies exist [6], [22], [23]. Dauphin et al designed a computational study of how the cilia motion and frequency affect the power output [23]. Their computation model of a ctenophore created higher power outputs at higher frequencies and longer waves of motion, which roughly agreed with previous data. Other research focuses on favorable conditions for the animals to generate thrust in fluid flows. The animals tended to rely on negative pressure fields around its cilia or paddles to generate thrust [24]. There are numerous benefits to the thrust generated from cilia, such as passive energy recapture, which ctenophores and other gelatinous animals use to swim efficiently [25]. Some ctenophores create vortices around their bodies to propel themselves in the desired direction [26]. This can be a very efficient method of swimming, especially since they are primarily drifters until they need to change direction or increase speed.

Though progress has been made in recent years, the swimming kinematics of ctenophores are still not well-understood. The water flume project sought to understand how beat frequency

of cilia is altered by ambient flow. The setup of this project was similar to one done by Barlow and Sleigh. In this project [27], the ctenophores were held stationary by a gripper apparatus. The beat frequency was also controlled using electromagnetic relays to trigger motion. They used the method of Particle Image Velocimetry (PIV, described in the next section) to measure the motion of the flow around the cilia. There was a very small flow through the tank in order to maintain water temperature (to eliminate as many factors to cilia motion as possible).

The turbulence tracking project has a similar mission to one done by Sutherland et al, who studied not only how the swimming mechanics of lobate ctenophores varied in turbulence, but also how feeding mechanics varied [7]. This study showed how a large group of animals were affected by different levels of artificially generated turbulence. The study showed that the animals reacted to increasing turbulence by changing their position in the tank, as well as increasing swimming velocities. Both projects aimed to understand ctenophore swimming mechanics. Understanding cilia (ctenes) and their motion is the first step to understanding the overall motion of ctenophore swimming mechanics.

Particle Image Velocimetry

We seek to measure the kinematics of the ctenes and the motion of the flow around them. One method of interest is Particle Image Velocimetry (PIV) [28]. PIV is a flow visualization technique in which the user illuminates small tracer particles and uses a high-speed camera or cameras to capture images of an area of interest. These images contain the illuminated particles, whose position over time is tracked in order to quantify their velocity. If the tracers are sufficiently small, the user may consider the tracer velocities as a proxy for the fluid velocity, thus noninvasively obtaining spatially and/or temporally resolved velocity fields of the background flow.

Previous research [29], [30] discusses how PIV can be applied to aquatic animals, including ctenophores [4], [26]. These applications are generally planar: a laser sheet is oriented perpendicular to the optical view of the high-speed camera, and an animal of interest swims through the viewing window (through tracer-seeded water). Commercial [31] or open-source (for example, [32]) algorithms are then used to calculate tracer displacements between subsequent frames, and eventually obtain velocity fields. From these velocity fields, one can calculate propulsive forces [33], wake dynamics [34], feeding currents [35], or other quantities of interest. Our project would have utilized a similar method of PIV (refer to Methods section for plans of PIV analysis in water flume project).

Project Goals

Despite the existence of previous studies on overall swimming dynamics [26] or cteno kinematics [6], there are still many as-yet unknown complexities to the motion of ctenophores. Their swimming mechanism is intriguing and unique among creatures of their size. The goal of the first research project was to fill the knowledge gap regarding the motion of ctenes in a (nonturbulent) background flow. We wanted to understand how different flow speeds affect cilia beat frequency and the length and duration of the strokes. The tank (and accompanying high-speed camera setup) was designed to allow users to accurately capture these data. This tank (described in the next section) is a water flume whose test section integrated a gripper apparatus to hold animals in place against an adjustable-speed background flow.

Only one previous study has investigated how animals' freely swimming behavior varies in turbulence [7]. There are still many questions to be asked about the effects of turbulence on these animals' behavior. For example, the distribution of the animals may change based on the amount of turbulence that is present. Another important question that we want to ask is how

swimming strategy (*e.g.* speed or geometry of swimming trajectories) might change in turbulent vs. still flow. We are also curious about how ctenophores control their position and orientation in increasing turbulence, and if there is a level of turbulence at which they lose this control.

Materials and Methods

Water Flume

Facility Construction

In order to measure animal swimming mechanics, a testing stage was necessary. This stage needed to be able to create its own current while holding the animals in place. A water flume is essentially a rectangular channel through which water flows at a controlled velocity [36]. Water flumes usually require a large flow loop with a separate test section and return line. Instead, we constructed a miniaturized “race track” style flume (Figure 4). The overall dimensions of the tank are 15”x7”x4.5”. The sides of the tank are ½” acrylic plastic. The top and bottom of the tanks are made of 1/8” acrylic and are removable, so a neoprene rubber gasket is required to make the seals watertight when these pieces are screwed on to the main tank body. The tank is separated into a test and return section with piece of 1/8” acrylic. The top section serves as the testing area while the bottom serves as the return area, where water circulates to re-enter the test section. Sections of PVC pipe are placed at both ends of the tank, serving as vanes to minimize flow separation. Water flow through the tank is driven by an adjustable-speed DC motor/impeller system. The impeller spins in the return section, driving flow to the top test section through a honeycomb straightener (which minimizes turbulence). While we were unable to make measurements of living animals in the tank due to the onset of the COVID-19 pandemic,

we designed specialized grippers to constrain the animals in the test section (Figure 5). Previous research used toothed plastic clamps for this purpose [27], while others used suction to tether the animal [37]. However, simple toothpicks have also shown to be effective means of attaching to gelatinous animals [38].

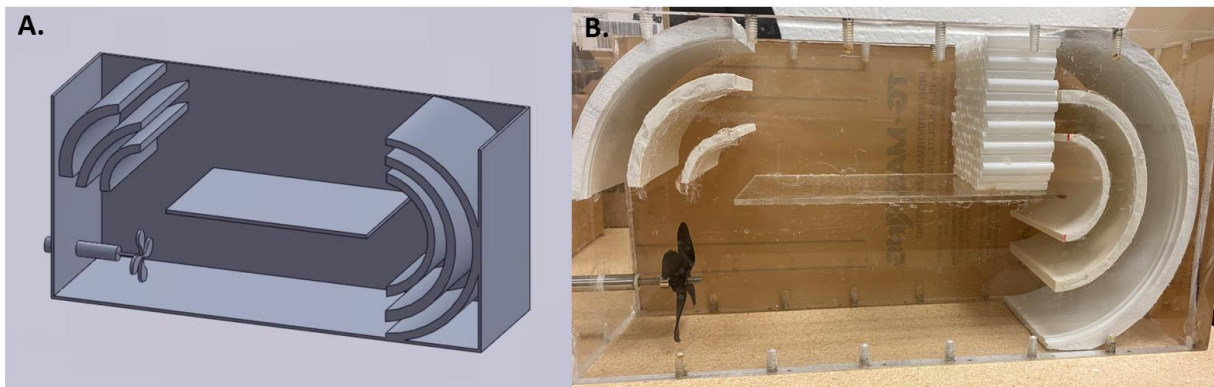


Figure 4. Water flume. [A] CAD model of miniature flume. [B] Fully built “race track” miniature flume, complete with impeller and honeycomb to mediate mean flow.

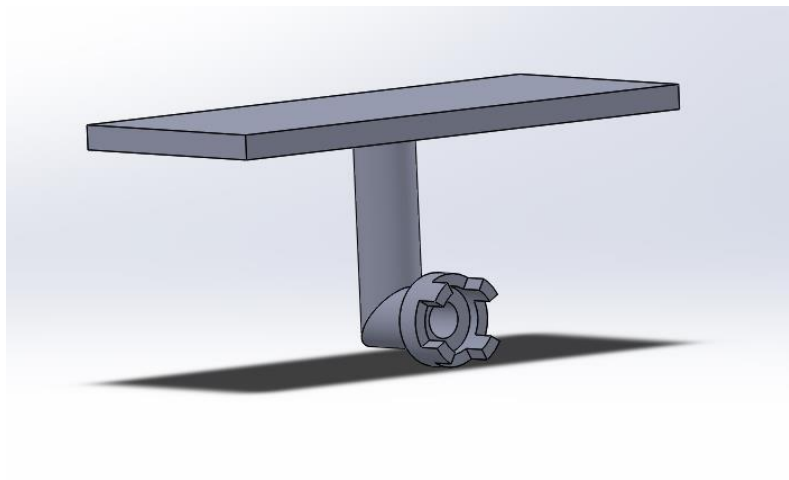


Figure 5. Gripper design. CAD model of potential four-pronged gripper, meant to be suspended from top of flume.

Preliminary Flow Data

In order to prepare for experiments, it was crucial to know what flow speeds could be produced in the flume and how the flow profile varied across the test section. The motor controller of the flume was set to 40%, 70%, and 100% to provide a low, medium, and high flow

speed. We imaged the test section using a high speed camera (Photron Fastcam AX200, Photron USA, Inc, San Diego, CA) focused, with a 55 mm lens (Micro-Nikkor, Nikon USA, Melville, NY), on the mid-plane of the test section. To provide a length reference for images, we placed a calibration plate in the focal plane of the camera (as shown in Figure 6) with markings every 2 cm. To quantify the flow, we placed small tracer particles (Sphericel, Potters Industries, Valley Forge, PA) measuring approximately $11\mu\text{m}$ into the water in the flume. To illuminate the tracers, we used a laser (4W continuous, 532nm, Laser Quantum, Fremont, CA) passing through a cylindrical lens, which created a sheet that shone through the bottom of the tank and into the testing area. Images were captured at a rate of 500 frames per second and analyzed and postprocessed using the MATLAB app, PIVlab [32]. Figure 7 shows an example set of preliminary flow data.

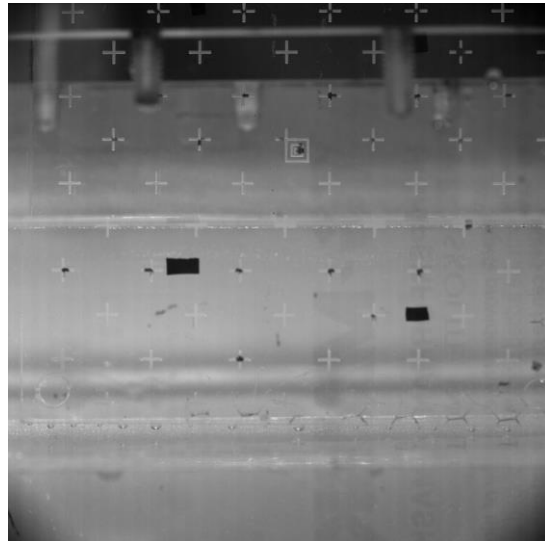


Figure 6. Calibration. Captured image of test area cross-section with calibration plate.

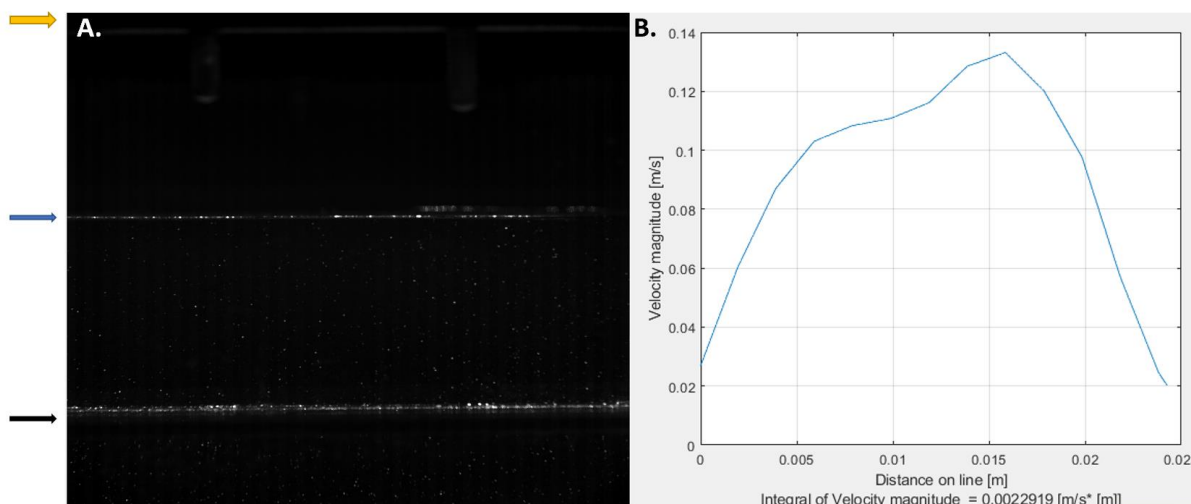


Figure 7. Water flume PIV. [A] Capture image of illuminated particles. Yellow arrow represents top of flume, blue arrow represents top of water level, and black arrow represents middle piece of acrylic separating the test and return sections. [B] Example of preliminary flow data. Y axis represents velocity magnitude. X axis represents the distance from the top of the middle section to the top of the water level (between the black arrows).

Turbulence Tracking

Turbulence tank

Due to the onset of the COVID-19 pandemic in March 2020, measurements of ctenophores in the water flume could not proceed as planned. This led to the second phase of the project, in which we analyzed the swimming behavior of ctenophores suspended in turbulence. These experiments were performed at the Monterey Bay Aquarium in June 2016 by Margaret Byron. The tank used for these experiments was a rectangular tank (Figure 8), which had underwater speakers mounted on the sides. These speakers, when actuated at low frequencies (30Hz) by an amplifier, were responsible for turbulence in the tank. For these experiments, the amplifier had three different settings: off (no flow), 0dB, 4dB, and 8dB. These corresponded to three different levels of turbulence and one still condition. The overall dataset consists of twelve videos, in three trials of each of the four turbulence settings. For each trial, about 15-20 ctenophores

(*Pleurobrachia bachei*) were placed in the tank and allowed to acclimate for 10 minutes at each amplifier setting.

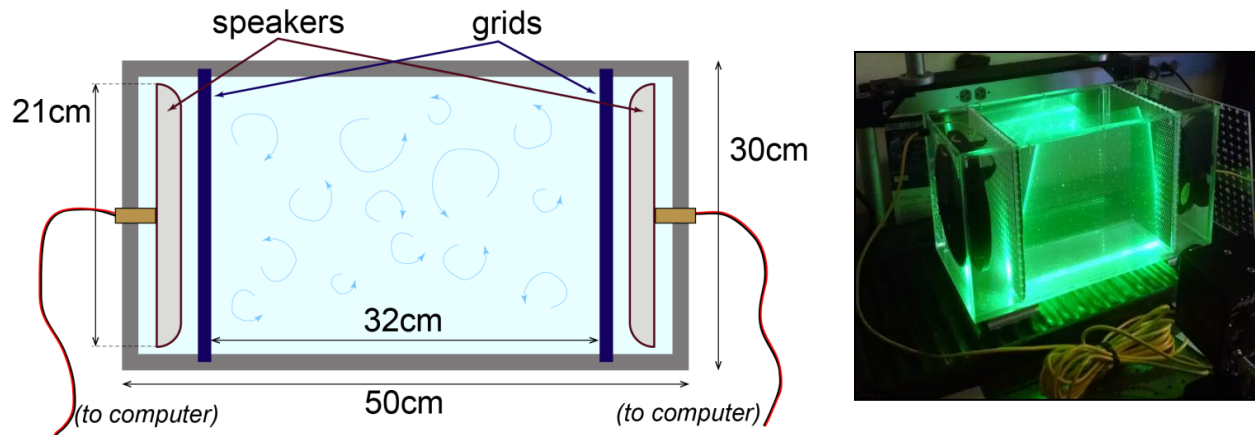


Figure 8. Turbulence tank. Speaker-driven turbulence tank (originally built by Kelly Sutherland and used in [7]). Right image shows laser illumination for PIV quantification of the turbulence in the tank, which is not discussed in this thesis. Figure courtesy of Margaret Byron.

Video Tracking

For each video, the animals were tracked using the MATLAB-based tool DLTdv8 [39]. In each video, the animals tended to remain close to the walls of the tank, but every so often would move away from the surrounding walls. These events were treated as “excursions”. These excursions were tracked from their beginning (defined as the start of motion away from wall) to their end (defined as the conclusion of motion back to the wall). Excursions were tracked for all twelve videos, with videos subsampled from 50fps (the original recording) to 5fps (reduced to ease the tracking burden). The tracked x and y position data was exported to serve as a training dataset for deep learning-based tracking of the 50fps videos.

Expansion and Analysis

As stated above, the original videos were taken at 50 fps, but the videos used for tracking were subsampled down to 5 fps. To expand the tracking to the full time resolution, the csv files containing the x-y positions were manipulated in MATLAB and mapped to 50fps time

resolution, with placeholder values (NaN) for the position in the untracked frames (see Appendix A). Using the neural network/deep learning capabilities of DLTdv8, we created datastores from these 50fps partially tracked datasets. Datastores are snapshots of all or part of a combined digitized point set and are used for training Deep Learning neural networks [40]. Using the datastores, a separate network can be trained for each recorded excursion. The trained networks can then be used to fully track individual animals at the 50 fps time resolution, overwrite the placeholder values with tracked data. Figure 9 shows the difference between the sparse data and fully tracked data.

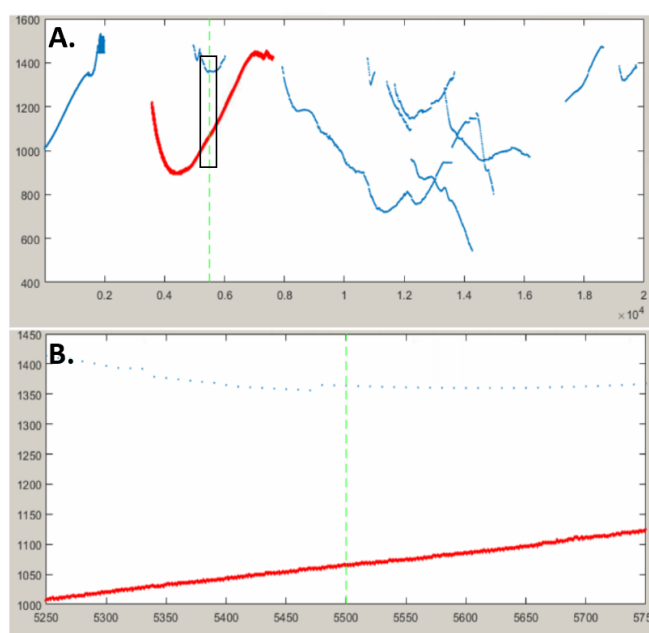


Figure 9. Tracked ctenophore positions. [A] shows the x positions of a tracked video. [B] shows a zoomed-in view of the x positions in the box shown in panel [A]. The blue set of data is the sparse data (5fps super sampled to 50fps) while the red is the fully tracked set of data after applying deep learning.

Using this approach, we obtain x-y positions for each excursion at 50fps. These two-dimensional data can then be calibrated to real space using an image of the same plate used for the water flume study. Seven videos (of twelve total) were expanded to 50fps time resolution

using this process; the process was time-intensive and we could not expand all twelve videos. The seven experiments were the full set of turbulence settings (still, 0dB, 4dB, 8dB) in trial 1 and the first three turbulence settings (still, 0dB, 4dB) of trial 3. Excursions for the still, 0dB, and 4dB conditions were grouped and analyzed as a single set, assuming that the trials (and each excursion within each trial) were independent. These combined datasets are labeled as turbulence level 0 to 3, matching respectively to the conditions of still to 8dB (for the 8dB data, only one video was analyzed). From these data sets (x-y positions of animals during “excursions”), we calculate derived quantities that give insight on the motion and swimming behavior of the animals. The code for this analysis can be seen in Appendix B.

Results

The results in this section are shown in box and whisker plots. The data used in box and whisker plots can be seen in the appropriate table in Appendix C. For each plot, red lines represent the median; the box extent represents the interquartile range (the 25th to 75th percentile); the whiskers indicate the nominal range of the data (1.5 times the interquartile range from the edges of the box); plus signs represent outliers; notches represent 95% confidence intervals on the median.

Excursion Duration

In this experiment, each excursion was roughly tracked from the moment the animal left any wall of the tank to when it returned to the wall of the tank. The beginning and endpoint of each excursion was determined by eye. We defined the duration of these excursions as the time (in seconds) elapsed from the beginning to the end of the tracked points. We can see in figure 10

that there may be a correlation between the excursion duration and the level of turbulence. As the level of turbulence rises, the duration of the excursions slightly increases. This is a very slight trend and is not statistically significant, but it indicates that further research on this topic may be worthwhile.

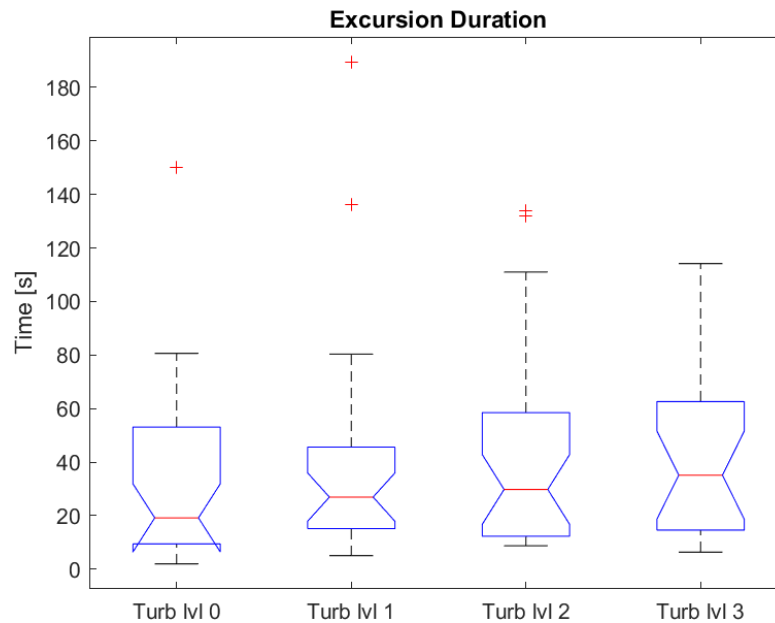


Figure 10. Excursion duration plots (data from table C-1)

Velocity

The velocity of the animals was calculated for each excursion using central differencing(see Appendix B). In figure 11, we can see both the average speed and maximum speed of each excursion. The plots show that there are no significant differences in the velocities across all the flow conditions, nor any visible trend in the median value. The average speed is more broadly distributed for the still and low-turbulence conditions than for the higher turbulence condition; however, this result is not significant. There is no noticeable difference between flow conditions for the maximum speed.

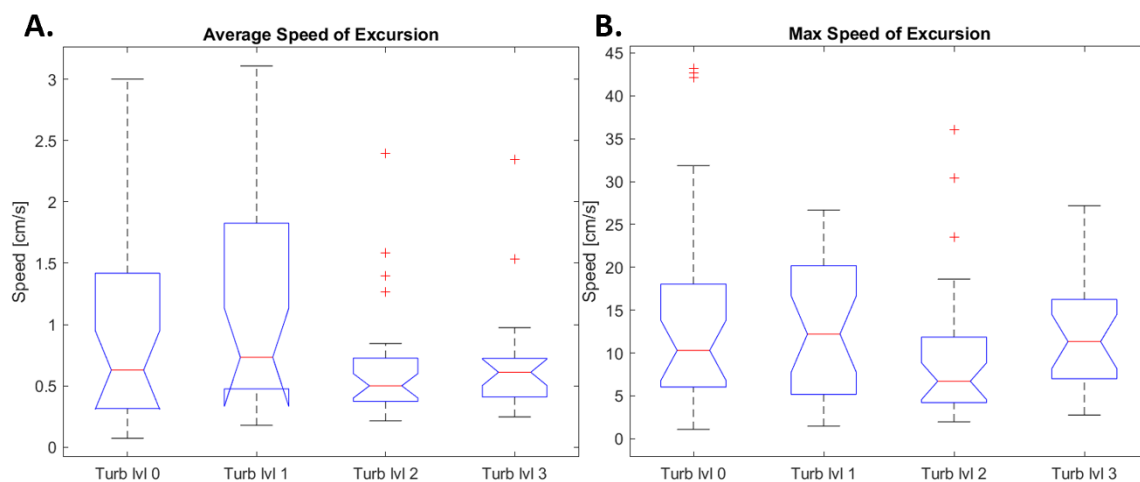


Figure 11. Plots for average and maximum speeds (data from table C-2)

Directionality

The directionality of the excursions was analyzed using two different methods: verticality and tortuosity. We defined verticality as the absolute value of each excursion's net vertical displacement divided by the net horizontal displacement. This ratio will be greatest when the animal has a much larger vertical displacement to horizontal displacement. The data for the net horizontal and vertical displacements is shown in figure 12. We can see that there are no major differences between flow conditions for either direction's net displacement. However, in considering the ratio of these two quantities (that is, the absolute value of the net y displacement divided by the absolute value of the net x displacement), we see an interesting pattern: the range of verticality is greater at lower turbulence levels (Figure 13). In the still condition, the animals favored more vertical excursions. However, as turbulence increased, the verticality decreases to near 1, meaning that trajectories are not preferentially oriented in either the vertical or horizontal directions. The results are not significant (95% confidence intervals overlap in each case) but further research is warranted.

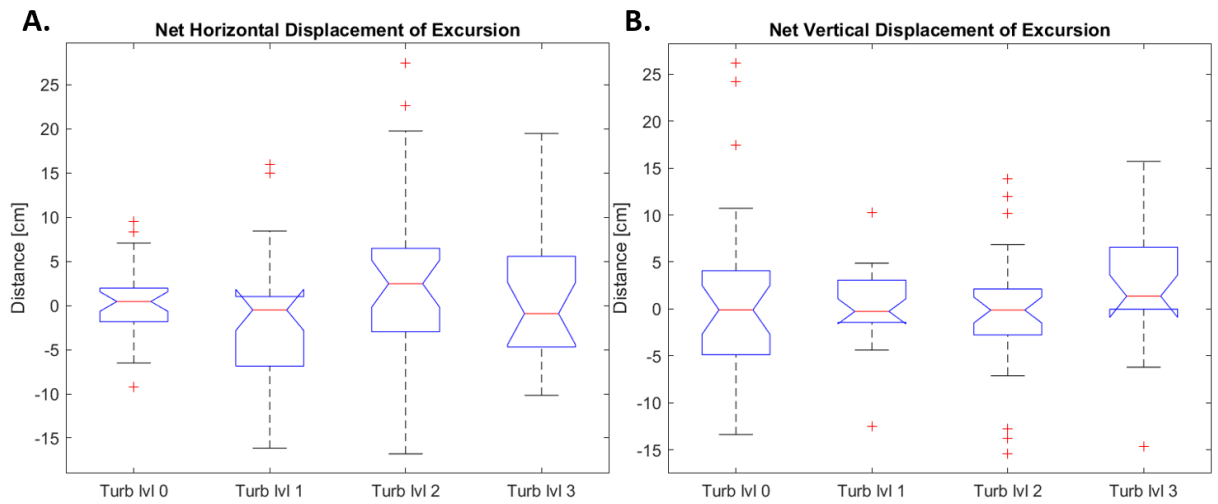


Figure 12. Net displacements. Net horizontal and vertical displacement for all excursions across all flow conditions (data from table C-3).

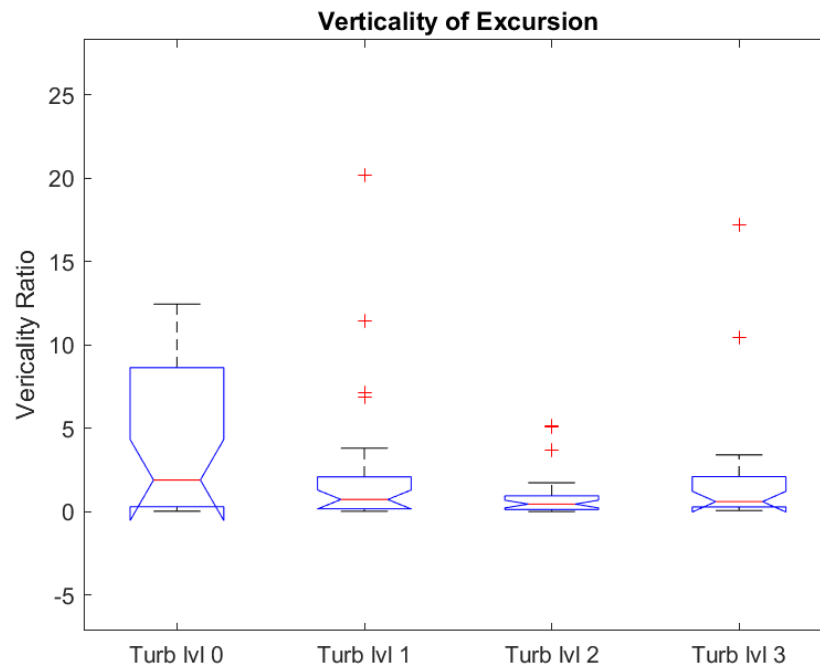


Figure 13. Verticality. Verticality of excursions (data from table C-4).

Tortuosity is a measure of how direct a path is and is defined as the length of the path divided by the shortest distance between the start and end points of the path. A very high tortuosity means the path is bendy and winding, while a tortuosity equal to one means the path is a straight line. We calculated each excursion's tortuosity by finding the displacement between each tracked point and then summing those displacements, then dividing by the total net displacement. The results are shown in Figure 14; there is no clear trend of tortuosity with turbulence level. Oddly, the very low turbulence level shows a higher tortuosity than either the still condition or the higher turbulence conditions. This is the only significant result of the analysis.

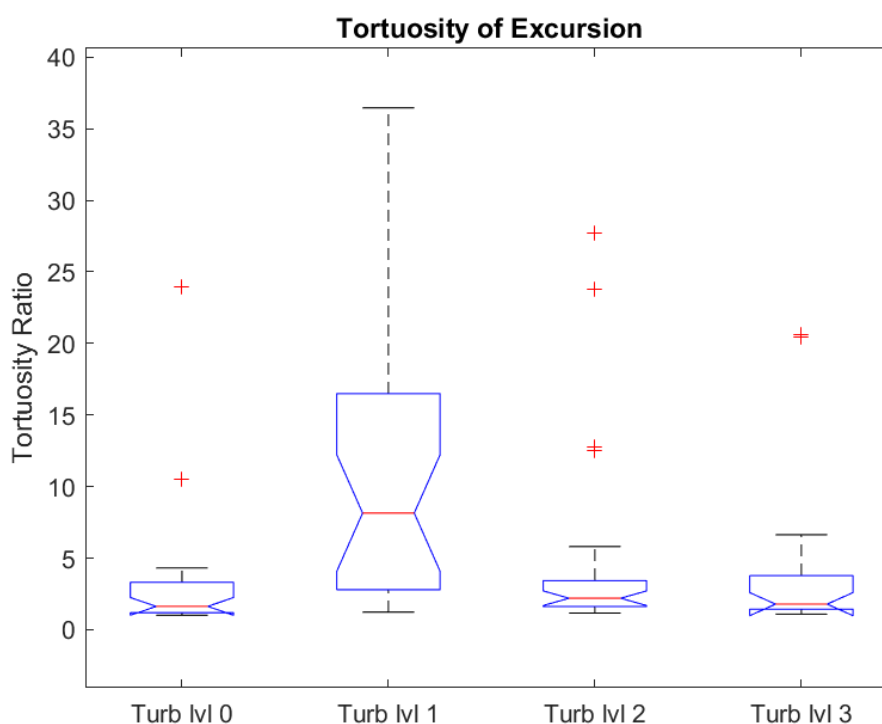


Figure 14. Tortuosity of excursions (data from table C-5).

Distribution

The distribution of the animals in the tank was not quantitatively compared between each experimental turbulence condition, since we tracked only the excursions of the animals and did

not track their positions otherwise. We therefore could not show that each excursion was performed by a different animal, and could not measure where animals drifted between excursions. However, we were able to compare the excursion paths and assumed distribution of the animals qualitatively. In figure 15, we can see all the tracked points of each excursion in each condition of the trial 3 group of animals. Here, there are clear differences in the path directionality and animal distribution as turbulence rises. It seems that as turbulence increases the animals tend to favor drifting to the top of the tank. However, the dataset is too small and not ideally measured to test this hypothesis. Further research is warranted.

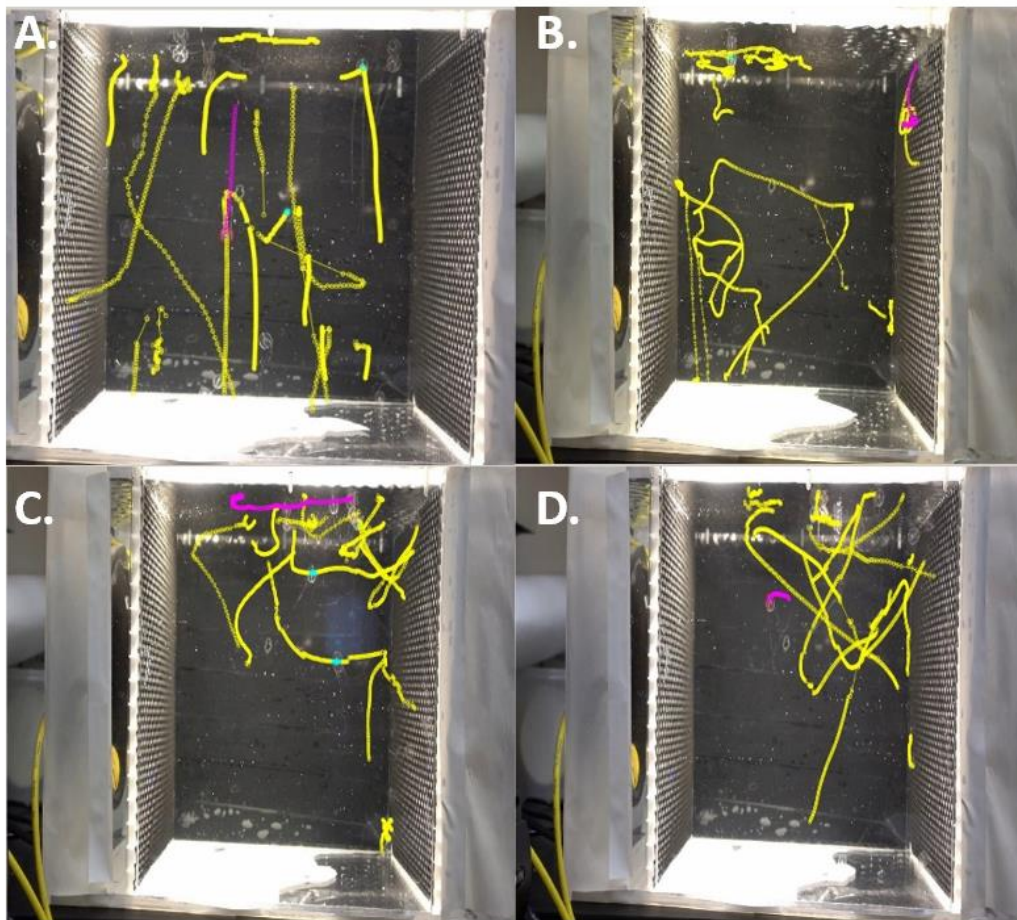


Figure 15. Excursion distribution. All tracked excursions for trial 3. [A] is the still condition, [B] is the 0dB condition, [C] is the 4dB condition, [D] is the 8dB condition.

Discussion and Conclusions

Two projects were discussed in the previous sections. Due to Covid-19 complications, the water flume project did not produce any results other than the initial flow validation/quantification. The preliminary flow data was within a desired range (10 cm/s – 30 cm/s) of speed. Future work on this project begins with gripping apparatus for the animals. Tests should be conducted with gelatinous subjects (even something as basic as a gummy bear) to see how the grippers would work on the ctenophore's body. It is important the gripping does not disrupt their ctenes rows. Further tests should be done to determine flow speed. The preliminary tests give a threshold of values, but lower settings on impeller should be explored to make sure flow speed remains under 30 cm/s. Once the facility is tested fully and functional, animal testing can begin. With proper calibration and PIV setup, we could capture images of the animals in a mean flow as originally planned, gaining more insight about their cilia and how ctenophores react to various flow speeds and even turbulence in their environment.

The second project, based on preexisting data, required a different type of analysis with its own challenges. The DLTdv8 tracking software was difficult to target precisely in more out-of-focus regions of the videos, and it was difficult to track the exact same point on the animal throughout its excursion. Additionally, the animals tended to cluster within the tank, making it difficult to tell which animal was which (since they are semi-transparent). This slowed the pace of the tracking. Taking all this into account, the method for tracking excursions was able to isolate the animals' swimming behavior away from the walls.

The excursion duration showed a slight increasing trend with increasing turbulence, with a slightly positive correlation with levels of turbulence and duration of excursion. However, the difference in values is not significant. The durations could be sensitive to human error. Despite a

high focus on accuracy, there is a large amount of experimenter dependence, since we determined by eye when the animal both left and returned to the wall. Further experiments can continue to test this possible correlation between duration of excursion and turbulence. It would be intriguing to see if turbulence can cause longer excursions because this would show us that the animals react to changes to flow around them. Longer excursions could mean that the animals are actively swimming against turbulent flows, since the flow may be extending the time it takes for them to return to the walls. Potentially, the reaction to turbulent flows even in the open ocean could be to actively swim against them, if they have motive such as returning to a location with more food.

The speeds of the excursions (average and maximum) did not change significantly with turbulence level. There is a lot of overlap between the values of the average and maximum speeds at different levels of turbulence, so turbulence may not affect the animals' ability to move at certain speeds. This tells us the animal is capable of maintaining speed regardless of the changes of flow in their environment. This could mean that the animal is capable of adapting its swimming to the turbulent effects it experiences. For stronger flows, it may be passively carried by them to maintain the same speed it would have gone if it was actively swimming. This is an example of efficient swimming mechanics that should be studied further.

The directionality of the excursions did depend on the flow condition, most dramatically in the verticality ratio. The verticality ratio represents the amount the animal traveled in a vertical direction as opposed to a horizontal direction. We saw that the spread of the verticality data was larger for lower values of turbulence: the paths of the animals became less vertical in increasing levels of turbulence. The range of verticality in the still condition was much greater than the higher levels of turbulence, and most values were above one (indicating that the trajectories were

more vertical than horizontal). However, as turbulence increased the verticality dropped towards a value of 1, indicating that animals tended to swim in both vertical and horizontal directions. It is possible that verticality decreased because animals were passively drifting with the turbulence. Seemingly in the still condition, the animals swim mostly up and down. In their natural habitat, this rise and fall through the water column could be their method of relocation. These animals would want to be in areas with an abundance of food and ideal temperatures. Turbulence can interfere with the verticality of their motion. In our experiment, the animals still went up and down, but added an element of horizontal motion. This could potentially help them to navigate the water column in turbulence.

The tortuosity calculation showed us a significant difference in lowest level of turbulence. We saw a clear distinction in values from the higher turbulent conditions to this lowest level of turbulence. It was also much greater than the value in the still condition. These results tell us that the animals take “bendier” paths for their excursions than other conditions. This could mean that the animals did not adjust for this low of a level of turbulence for their swimming paths. The still condition has low tortuosity so the animal is taking straight paths. So potentially, the ctenophore may be trying to take the same path in the lowest turbulent conditions while not making adjustments to its swimming behavior. In their natural habitat, they experience different levels of turbulence frequently. It is possible that ctenophores react only to certain levels of turbulence since it may be inefficient to actively swim against stronger flows.

We were not able to definitively calculate the spatial distribution of the animals, because we focused only on the excursions through the center of the tank and did not track animals between excursions. However, when we look at the excursions qualitatively, we see a pattern: animals swam closer to the top of the tank as turbulence increased. This could be the animal's

response to avoiding turbulence. The turbulence was throughout the tank, but the ctenophores would likely experience it much more in the middle and bottom of the tank. Rising to the top of the tank could be the animal's response to remove itself from a turbulent environment, or at least minimize its effects.

The data show that ctenophores' active swimming patterns, which we quantify using excursions through the center of our tank, are mildly affected by turbulence. As turbulence increased, we did not see much change in factors like net displacement or swimming speed, but did observe potential trends in verticality, tortuosity, and duration of excursions. Future work will include continuing the data analysis to all twelve videos to draw further conclusions about the ctenophores' behavior in turbulence. This future work can also increase statistical power and may confirm the potential patterns we have discussed. The excursions tracked here are two-dimensional projections; future experiments could use multiple cameras to observe 3D trajectories, literally adding a new dimension to the analysis.

Appendix A

Expansion Code

```
q1 = readmatrix('DLTdv8_data_xypts.csv');
i1= size(q1,1);
B1=[reshape(q1,1,[]);nan(9,numel(q1))];
B1=B1(:);
d1 = reshape(B1,i1+9*i1,[]);
writematrix(d1,'DLTdv8_data_expanded_xypts.csv');

q2 = readmatrix('DLTdv8_data_xyzpts.csv');
i2= size(q2,1);
B2=[reshape(q2,1,[]);nan(9,numel(q2))];
B2=B2(:);
d2 = reshape(B2,i2+9*i2,[]);
writematrix(d2,'DLTdv8_data_expanded_xyzpts.csv');

q3 = readmatrix('DLTdv8_data_offsets.csv');
i3= size(q3,1);
B3=[reshape(q3,1,[]);zeros(9,numel(q3))];
B3=B3(:);
d3 = reshape(B3,i3+9*i3,[]);
writematrix(d3,'DLTdv8_data_expanded_offsets.csv');

q4 = readmatrix('DLTdv8_data_xyzres.csv');
i4= size(q4,1);
B4=[reshape(q4,1,[]);nan(9,numel(q4))];
B4=B4(:);
d4 = reshape(B4,i4+9*i4,[]);
writematrix(d4,'DLTdv8_data_expanded_xyzres.csv');
```

Appendix B

Excursion Analysis Code

```

%-----
% CTENOTRACKER
%-----
% This code analyzes 2D tracked data from swimming ctenophores in the
% rectangular turbulence tank (collected June 2016)
%-----
% Authors: Carlos Abarca and Margaret Byron
% Date: May 2021
%-----

clear all
close all
%%
%-----STEP ONE: FILE STORAGE-----
maindir='C:/users/cabar/desktop/final_dlt_points'; %This is where the CSV
files containing tracked points are

%useful variables
fps=50; %fps
T1_cal=30.0665; %px/cm
T3_cal=29.069; %px/cm
T1_top=36/T1_cal; %cm
T1_bottom=1030/T1_cal; %cm
T3_top=24/T3_cal; %cm
T3_bottom=1034/T3_cal; %cm

% [This is where the code will go to read in CSV files while preserving
% their organization]

filePattern = fullfile(maindir, '*.csv');
csvFiles = dir(filePattern);

for N_file = 1:length(csvFiles)
    baseFileName = csvFiles(N_file).name;
    fullFileName = fullfile(maindir, baseFileName);
    [filepath,name,ext]=fileparts(fullFileName);
    names{N_file}=[name];
    fprintf(1, 'Now reading %s\n', fullFileName);

    DATA=readmatrix(fullFileName);

%How many excursions are there in this file???
    N_ex=size(DATA,2)/2;

%Main loop for each CSV file: 1 to N_ex excursions
for ex=1:N_ex
    %extract the two columns that make up the (X,Y) coordinates of this
excursion
    temp=DATA(:,2*ex-1:2*ex); %Extract the columns for current excursion

```

```

curr_ex=rmmmissing(temp); %Remove the NaNs which are padding the current
excursion

%[code which stores the time data for the excursion]
t = ~isnan(temp(:,1));
time = find(t == 1);
t_stamps{ex,N_file}=time./(fps); %reports frame numbers where values
appear

%Option 1: cell array
if N_file<=4
    XY_excursions{ex,N_file}=curr_ex./(T1_cal); %Store current excursion
coordinates in cell array
else
    XY_excursions{ex,N_file}=curr_ex./(T3_cal);
end

end

end

%%
%-----STEP TWO: ANALYSIS-----
for j=1:size(XY_excursions,2) %Loop through all trials
    for i=1:size(XY_excursions,1) %Loop through all exc.s within each trial
        if isempty(XY_excursions{i,j})%skips over empty rows to continue with
analysis
            continue
        end
        curr_ex=XY_excursions{i,j}; %current XY coords in cm
        curr_t=t_stamps{i,j};

        %Duration of each excursion
        Ex_size=size(curr_ex,1)./fps;
        Ex_duration{i,j}=[Ex_size];

        %Central differencing of position to obtain velocity
        u_diff=diff(curr_ex(2:end,1))+diff(curr_ex(1:end-1,1));
        v_diff=diff(curr_ex(2:end,2))+diff(curr_ex(1:end-1,2));
        t_diff=diff(curr_t(2:end,1))+diff(curr_t(1:end-1,1));
        u_vel=u_diff./t_diff;
        v_vel=v_diff./t_diff;

        %Calculate velocities of animals in each excursion, along with
        %maximum and average speed
        Ex_Vels{i,j}=[u_vel v_vel];
        Avg_speed{i,j}=nanmean((u_vel.^2+v_vel.^2).^0.5);
        Max_speed{i,j}=nanmax((u_vel.^2+v_vel.^2).^0.5);
        curr_speed=((u_vel.^2+v_vel.^2).^0.5);

        %Extract intial and final x&y position of each excursion
        x_final=curr_ex(end,1);
        x_init=curr_ex(1,1);
        y_final=curr_ex(end,2);

```

```

y_init=curr_ex(1,2);
%[calculate net x&y displacement]
net_x=x_final-x_init;
net_y=y_final-y_init;
Net_horz{i,j}=[net_x];
Net_vert{i,j}=[net_y];
%Verticality ratio
Verticality{i,j}=[abs(net_y)/abs(net_x)];

%Define path tortuosity
net_disp=norm(curr_ex(end,:)-curr_ex(1,:));
step_disp=0;
for k=2:length(curr_ex)
    step_disp(k)=norm(curr_ex(k,:)-curr_ex(k-1,:));
end
total_disp=nansum(step_disp);
Tortuosity{i,j}=total_disp/net_disp;
clear net_disp step_disp total_disp

end
end

%%
%-----STEP THREE: BOXPLOTS-----

s=sum(~cellfun(@isempty,Ex_duration),1);
n1= repmat('Turb lvl 0',s(1)+s(2),1);
n2= repmat('Turb lvl 1',s(3)+s(4),1);
n3= repmat('Turb lvl 2',s(5)+s(6),1);
n4= repmat('Turb lvl 3',s(7),1);
n=[n1;n2;n3;n4];
x1=vertcat(Ex_duration{:});
x2=vertcat(Avg_speed{:});
x3=vertcat(Max_speed{:});
x4=vertcat(Net_horz{:});
x5=vertcat(Net_vert{:});
x6=vertcat(Verticality{:});
x7=vertcat(Tortuosity{:});

boxplot(x1,n,'Notch','on')
title('Excursion Duration')
ylabel('Time [s]')
pause

boxplot(x2,n,'Notch','on')
title('Average Speed of Excursion')
ylabel('Speed [cm/s]')
pause

boxplot(x3,n,'Notch','on')
title('Max Speed of Excursion')
ylabel('Speed [cm/s]')
pause

boxplot(x4,n,'Notch','on')

```

```
title('Net Horizontal Displacement of Excursion')  
ylabel('Distance [cm]')  
pause
```

```
boxplot(x5,n,'Notch','on')  
title('Net Vertical Displacement of Excursion')  
ylabel('Distance [cm]')  
pause
```

```
boxplot(x6,n,'Notch','on')  
title('Verticality of Excursion')  
ylabel('Verticality Ratio')  
pause
```

```
boxplot(x7,n,'Notch','on')  
title('Tortuosity of Excursion')  
ylabel('Tortuosity Ratio')
```

Appendix C

Data Tables

Table C-1. Data of excursion duration (units in seconds)

Turbulence Level 0 (still)	Turbulence Level 1 (0dB)	Turbulence Level 2 (4dB)	Turbulence Level 3 (8dB)
61.42	39.64	18.38	29.68
5.7	80.36	97.9	53.42
10.18	22.38	59.12	13.62
18.62	136.2	38.04	17.08
26.16	7.22	55.74	49.96
19.16	17.12	8.86	93.36
6.86	39.1	131.84	8.88
11.26	36.82	133.94	77.28
7.24	50.66	106.6	88.64
1.98	23.52	10.04	16.84
22.52	11.7	111.02	49.16
12.42	66.02	84.02	11.06
77.4	5.06	22.98	35.12
20.3	52.12	19.96	64.92
13.42	15.56	8.74	6.36
5.76	16.38	10.48	10.86
78.34	189.48	29.78	114.16
13.58	22.2	40.18	38.1
18.24	35.46	12.22	21.9
59.54	14.76	12.58	14.92
21.52	40.54	9.06	61.82
34.6	7.46	10.84	
77.96	11.42	56.58	

80.62	136.26	42.62	
150.02	8.16	51.36	
50.92	17.48	13.46	
7.26	36.94	9.78	
41.86	30.34	20.2	
6.62		31.98	
		16.02	
		67.16	

Table C-2. Data of average and maximum speeds (units in centimeter/second)

Turbulence Level 0 (still)		Turbulence Level 1 (0dB)		Turbulence Level 2 (4dB)		Turbulence Level 3 (8dB)	
Average	Max	Average	Max	Average	Max	Average	Max
0.410341	12.40504	3.107673	70.90693	0.323387	6.518365	0.635395	14.2381
1.394999	29.65457	1.696536	15.51687	0.424257	6.980598	0.423359	8.024053
1.817238	9.798906	1.604153	11.8177	0.54801	5.186001	0.699871	13.24239
0.358092	19.09527	2.254408	24.29896	0.500529	11.47126	0.337032	4.455316
0.188967	5.850218	2.140928	18.06285	0.467984	9.882084	0.247432	4.928463
0.4635	17.6854	2.000959	13.60691	1.263636	12.6346	0.610942	14.22634
1.769681	42.11054	0.948358	10.70649	0.301887	4.349974	0.974346	3.319654
0.677229	12.80603	2.486568	22.44678	0.438936	6.706468	0.257883	11.33291
0.52158	6.085946	1.948752	20.8548	0.321723	8.056008	0.412682	20.1274
3.00032	43.19351	1.44216	8.200165	2.393773	12.57611	0.796993	8.257244
0.795466	31.8596	2.214686	12.36099	0.366506	30.37214	0.624505	14.94969
1.912943	25.00467	1.613421	26.67325	0.606087	7.036359	0.663629	7.161573
0.133159	3.069562	1.70277	12.69215	1.585907	18.62302	0.673403	6.515431

1.255014	8.589491	0.442434	19.51766	0.845512	17.29563	0.401141	8.690762
1.851168	15.25556	0.562381	23.71709	0.606772	3.595889	2.344128	14.03242
0.913962	8.634492	0.409543	3.869756	0.575422	2.429499	1.534774	26.43582
0.096905	1.09106	0.382638	47.39273	0.733194	36.02191	0.596764	23.69993
0.519443	13.95497	0.359381	10.05346	0.41078	7.886335	0.435258	27.183
0.631157	10.30147	0.374129	1.48846	0.215029	3.290388	0.497829	24.13617
0.072686	1.451397	0.544373	15.2368	0.839995	4.397753	0.809106	10.52373
1.487638	15.54028	0.550386	4.786041	1.395395	4.713718	0.359308	2.763351
0.37188	9.980532	0.745265	3.238777	0.394597	1.97665		
0.422185	12.62417	0.720707	2.924293	0.644697	11.97256		
0.102654	8.414718	0.530851	5.550013	0.672575	23.47891		
0.105307	1.427962	0.508284	2.28886	0.423048	2.046177		
0.188771	2.280118	0.350311	8.164391	0.704835	3.116844		
0.935046	6.347675	0.178092	1.46901	0.831956	8.116911		
0.629014	42.69753	0.520192	12.05197	0.296963	4.687662		
1.643795	2.576412			0.286674	4.00003		
				0.349623	4.92066		
				0.398253	4.171243		

Table C-3. Data of net horizontal and vertical displacement (units in centimeters)

Turbulence Level 0 (still)		Turbulence Level 1 (0dB)		Turbulence Level 2 (4dB)		Turbulence Level 3 (8dB)	
Horz.	Vert.	Horz.	Vert.	Horz.	Vert.	Horz.	Vert.
-6.5086	0.842574	15.99212	-0.44367	-3.28651	0.251885	-4.80018	2.843726

-6.10086	-1.11261	7.486714	1.377784	-3.46369	-0.18823	-1.16225	0.133521
-5.88244	0.630082	-1.74793	-12.5011	22.59842	10.14202	-1.07812	1.188869
-2.87053	-1.45984	-15.6931	3.344903	4.964972	-7.10226	-4.66003	1.105362
0.528746	-4.61934	-2.86033	3.489235	12.06703	-2.91488	-10.1658	1.358936
2.81025	-0.77312	-7.54545	-0.10108	3.636701	-0.37853	15.38013	10.54189
-2.56835	1.774772	-13.1209	-1.15969	27.4565	5.0699	-8.08439	0.473148
0.727399	-6.3999	0.035524	-0.40686	14.76613	13.86525	4.101419	13.93598
0.656287	-1.01829	-9.63134	0.234488	1.294595	-0.32394	-1.20189	12.57305
0.493943	-5.80648	8.436679	4.873511	4.171239	-15.4159	0.46493	-0.48443
9.557081	-0.73018	-0.98836	-1.70567	-8.60648	-5.94083	19.47603	1.720277
2.382711	10.18877	14.93775	10.2436	-16.791	-13.7737	3.45519	1.310143
3.651548	-5.74278	1.123117	0.850778	-16.3961	-12.7556	2.89094	-5.9153
-9.24412	17.47953	0.792085	1.34167	3.80183	-4.76448	18.23147	5.254596
2.81601	24.15761	-6.19252	-1.59965	-4.70997	-0.51238	4.81534	10.72864
0.451813	4.881935	0.904057	-0.95164	2.466791	-1.54733	-8.79116	-4.7483
1.266078	-6.59118	-8.52901	2.799638	2.327946	11.97382	-5.1188	-14.6696
-0.04206	-5.81417	-3.86643	0.500681	0.784635	0.224347	8.369494	3.404666
-0.51825	3.790281	0.369914	-0.60779	-0.78749	-0.11601	7.83087	2.500514
1.822633	-0.52916	0.18411	3.712941	6.58065	-0.0999	-4.07393	-6.19048
7.071673	26.17955	-16.1482	-1.25735	-8.09375	-1.30005	-0.91214	15.70975
-1.71007	2.796541	1.146101	4.353358	-0.45673	2.308407		
-2.2013	2.340134	0.442988	-3.04367	-5.99472	-2.67585		
0.450888	-5.60883	-7.52688	3.852205	19.75476	6.842518		
-1.55576	-13.3701	-3.54585	-0.49216	15.73834	1.58299		

8.367308	0.163537	-2.26948	-2.5174	6.146812	5.791058		
-1.37263	6.082503	-0.01931	-1.72602	4.086903	4.616875		
-1.13105	-0.09353	1.797783	-4.37847	-2.01043	-0.07621		
-0.92124	10.71805			3.600104	-2.79617		
				-0.26552	0.457825		
				14.61537	-0.00998		

Table C-4. Data of Verticality

Turbulence Level 0 (still)	Turbulence Level 1 (0dB)	Turbulence Level 2 (4dB)	Turbulence Level 3 (8dB)
0.129455	0.027743	0.076642	0.592421
0.182369	0.184031	0.054345	0.114881
0.107112	7.15193	0.448793	1.102725
0.50856	0.213145	1.430473	0.237201
8.73642	1.219873	0.241558	0.133677
0.275107	0.013396	0.104087	0.685423
0.691017	0.088385	0.184652	0.058526
8.798336	11.45333	0.93899	3.397844
1.551593	0.024346	0.250222	10.46102
11.75537	0.577657	3.695762	1.041945
0.076402	1.725759	0.690274	0.088328
4.276127	0.685753	0.820302	0.379181
1.572697	0.757515	0.777964	2.046153
1.890881	1.693845	1.253207	0.288216
8.578664	0.25832	0.108786	2.228012
10.8052	1.052638	0.627263	0.540122
5.205983	0.328249	5.143514	2.865831

138.2284	0.129494	0.285926	0.406795
7.313647	1.643051	0.147318	0.319315
0.290326	20.16699	0.015181	1.519537
3.702031	0.077863	0.160624	17.22297
1.635339	3.798407	5.054233	
1.063071	6.870765	0.446368	
12.43951	0.511793	0.346373	
8.593986	0.138799	0.100582	
0.019545	1.109239	0.942124	
4.431271	89.39535	1.129676	
0.082697	2.435482	0.037906	
11.63438		0.77669	
		1.724278	
		0.000683	

Table C-5. Data of tortuosity

Turbulence Level 0 (still)	Turbulence Level 1 (0dB)	Turbulence Level 2 (4dB)	Turbulence Level 3 (8dB)
3.934953	16.98724	2.100655	3.951528
1.305302	36.07514	12.72944	20.48891
3.16753	6.268526	1.389824	6.638174
2.142216	36.46042	2.397985	1.249513
1.12727	5.568499	2.203457	1.31044
3.517836	8.5829	3.273719	3.21625
4.317034	6.885795	1.512626	1.092641
1.208173	476.3262	3.096464	1.548833
3.246604	22.09689	27.6797	3.010763
1.0708	7.723096	1.52751	20.64764

3.814016	28.09666	4.169956	1.659988
2.345819	12.749	2.423097	2.112198
1.752733	11.48511	1.836987	3.733353
1.314909	16.00715	3.113473	1.466071
1.028276	1.559368	1.163937	1.277246
1.090265	9.296304	2.450504	1.790908
1.179737	8.967876	2.071738	4.603287
1.262053	2.499001	23.7677	1.949826
3.101347	20.61655	3.768155	1.391911
2.660317	2.612571	1.699897	1.781189
1.196508	1.514155	1.619101	1.455081
4.138461	1.326325	2.029814	
10.50951	2.986768	5.813234	
1.633631	9.141688	1.536642	
1.229844	1.233139	1.632996	
1.197538	1.974116	1.228304	
1.103337	7.170202	1.436115	
23.93977	5.334137	3.484875	
1.016609		2.242907	
		12.51901	
		2.201995	

Works Cited

- [1] M.-L. Hernandez-Nicaise, “Ctenophora,” in *Microscopic Anatomy of Invertebrates, Volume 2: Placozoa*, 1991, pp. 359–418.
- [2] S. L. Tamm, “Cilia and the life of ctenophores,” *Invertebr. Biol.*, vol. 133, no. 1, pp. 1–46, Mar. 2014, doi: 10.1111/ivb.12042.
- [3] H. Machemer, “Ciliary Activity and the Origin of Metachrony in Paramecium: Effects of Increased Viscosity,” *J. Exp. Biol.*, vol. 57, no. 1, pp. 239–259, 1972.
- [4] W. L. Heimbichner Goebel, S. P. Colin, J. H. Costello, B. J. Gemmell, and K. R. Sutherland, “Scaling of ctenes and consequences for swimming performance in the ctenophore *Pleurobrachia bachei*,” *Invertebr. Biol.*, vol. 139, no. 3, p. e12297, Aug. 2020, doi: 10.1111/ivb.12297.
- [5] G. I. Matsumoto, “Swimming movements of ctenophores, and the mechanics of propulsion by ctene rows,” *Hydrobiologia*, vol. 216–217, no. 1, pp. 319–325, Jun. 1991, doi: 10.1007/BF00026481.
- [6] W. L. Heimbichner Goebel, S. P. Colin, J. H. Costello, B. J. Gemmell, and K. R. Sutherland, “Scaling of ctenes and consequences for swimming performance in the ctenophore *Pleurobrachia bachei*,” *Invertebr. Biol.*, vol. 139, no. 3, pp. 1–9, 2020, doi: 10.1111/ivb.12297.
- [7] K. R. Sutherland, J. H. Costello, S. P. Colin, and J. O. Dabiri, “Ambient fluid motions influence swimming and feeding by the ctenophore *Mnemiopsis leidyi*,” *J. Plankton Res.*, vol. 36, no. 5, pp. 1310–1322, Sep. 2014, doi: 10.1093/plankt/fbu051.
- [8] F. G. Michalec, I. Fouxon, S. Souissi, and M. Holzner, “Zooplankton can actively adjust their motility to turbulent flow,” *Proc. Natl. Acad. Sci. U. S. A.*, vol. 114, no. 52, pp.

- E11199–E11207, Dec. 2017, doi: 10.1073/pnas.1708888114.
- [9] T. Kiørboe and E. Saiz, “Planktivorous feeding in calm and turbulent environments, with emphasis on copepods,” *Mar. Ecol. Prog. Ser.*, vol. 122, no. 1–3, pp. 135–145, Jun. 1995, doi: 10.3354/meps122135.
- [10] J. C. Prairie, K. R. Sutherland, K. J. Nickols, and A. M. Kaltenberg, “Biophysical interactions in the plankton: A cross-scale review,” *Limnol. Oceanogr. Fluids Environ.*, vol. 2, no. 1, pp. 121–145, Apr. 2012, doi: 10.1215/21573689-1964713@10.1002/(ISSN)1541-5856.ECODAS-VI.
- [11] B. Gaylord, J. Hodin, and M. C. Ferner, “Turbulent shear spurs settlement in larval sea urchins,” *Proc. Natl. Acad. Sci. U. S. A.*, vol. 110, no. 17, pp. 6901–6906, Apr. 2013, doi: 10.1073/pnas.1220680110.
- [12] M. R. A. Koehl, “Mini review: Hydrodynamics of larval settlement into fouling communities,” *Biofouling*, vol. 23, no. 5. Taylor & Francis , pp. 357–368, Oct. 2007, doi: 10.1080/08927010701492250.
- [13] “Ctenophore | marine invertebrate | Britannica.”
<https://www.britannica.com/animal/ctenophore> (accessed Jun. 09, 2021).
- [14] S. H. D. Haddock, “A golden age of gelata: Past and future research on planktonic ctenophores and cnidarians,” in *Hydrobiologia*, Nov. 2004, vol. 530–531, pp. 549–556, doi: 10.1007/s10750-004-2653-9.
- [15] G. H. Parker, “The movements of the swimming-plates in ctenophores, with reference to the theories of ciliary metachronism,” *J. Exp. Zool.*, vol. 2, no. 3, pp. 407–423, Aug. 1905, doi: 10.1002/jez.1400020306.
- [16] B. A. Afzelius, “The fine structure of the cilia from ctenophore swimming-plates.,” *J.*

- Biophys. Biochem. Cytol.*, vol. 9, no. 2, pp. 383–94, Feb. 1961, doi: 10.1083/JCB.9.2.383.
- [17] S. L. Tamm, “Mechanical synchronization of ciliary beating within comb plates of ctenophores,” *J. Exp. Biol.*, vol. 113, pp. 401–408, 1984, doi: 10.1242/jeb.113.1.401.
- [18] S. L. Tamm, “Mechanisms of ciliary coordination in ctenophores,” *J. Exp. Biol.*, vol. 59, no. 1, pp. 231–245, 1973, doi: 10.1242/jeb.59.1.231.
- [19] J. R. Blake and M. A. Sleight, “Mechanics of ciliary locomotion,” *Biol. Rev.*, vol. 49, no. 1, pp. 85–125, Feb. 1974, doi: 10.1111/j.1469-185X.1974.tb01299.x.
- [20] D. Barlow and M. A. Sleight, “Water propulsion speeds and power output by comb plates of the ctenophore *Pleurobrachia pileus* under different conditions,” *J. Exp. Biol.*, vol. 183, no. 1, 1993.
- [21] C. Brennen and H. Winet, “Fluid Mechanics of Propulsion by Cilia and Flagella,” *Annu. Rev. Fluid Mech.*, vol. 9, no. 1, pp. 339–398, Jan. 1977, doi: 10.1146/annurev.fl.09.010177.002011.
- [22] G. I. Matsumoto and W. M. Hamner, “Modes of water manipulation by the lobate ctenophore *Leucothea* sp.,” *Mar. Biol.*, vol. 97, no. 4, pp. 551–558, Apr. 1988, doi: 10.1007/BF00391051.
- [23] A. Dauptain, J. Favier, and A. Bottaro, “Hydrodynamics of ciliary propulsion,” *J. Fluids Struct.*, vol. 24, no. 8, pp. 1156–1165, Nov. 2008, doi: 10.1016/J.JFLUIDSTRUCTS.2008.06.007.
- [24] S. P. Colin, J. H. Costello, K. R. Sutherland, B. J. Gemmell, J. O. Dabiri, and K. T. Du Clos, “The role of suction thrust in the metachronal paddles of swimming invertebrates,” *Sci. Rep.*, vol. 10, p. 17790, 2020, doi: 10.1038/s41598-020-74745-y.
- [25] B. J. Gemmell, J. H. Costello, S. P. Colin, C. J. Stewart, J. O. Dabiri, D. Tafti, and S.

- Priya, “Passive energy recapture in jellyfish contributes to propulsive advantage over other metazoans,” *Proc. Natl. Acad. Sci. U. S. A.*, vol. 110, no. 44, pp. 17904–17909, Oct. 2013, doi: 10.1073/pnas.1306983110.
- [26] B. J. Gemmell, S. P. Colin, J. H. Costello, and K. R. Sutherland, “A ctenophore (comb jelly) employs vortex rebound dynamics and outperforms other gelatinous swimmers,” doi: 10.1098/rsos.181615.
- [27] D. Barlow, M. A. Sleigh, and R. J. White, “Water flows around the comb plates of the ctenophore *Pleurobrachia* plotted by computer: a model system for studying propulsion by antiplectic metachronism,” *J. Exp. Biol.*, vol. 177, no. 1, 1993.
- [28] M. Raffel, C. E. Willert, F. Scarano, C. J. Kähler, S. T. Wereley, and J. Kompenhans, *Particle Image Velocimetry: A Practical Guide*. Springer International Publishing, 2018.
- [29] E. J. Stamhuis and J. J. Videler, “Quantitative flow analysis around aquatic animals using laser sheet particle image velocimetry,” *J. Exp. Biol.*, vol. 198, no. 2, pp. 283–294, Feb. 1995, doi: 10.1242/jeb.198.2.283.
- [30] B. J. Gemmell, H. Jiang, and E. J. Buskey, “A new approach to micro-scale particle image velocimetry (μ PIV) for quantifying flows around free-swimming zooplankton,” *J. Plankton Res.*, vol. 36, no. 5, pp. 1396–1401, Sep. 2014, doi: 10.1093/plankt/fbu067.
- [31] “Microvec PIV Software – Microvec Pte Ltd.” <https://piv.com.sg/piv-products/microvec-piv-software/> (accessed Jun. 09, 2021).
- [32] W. Thielicke and E. J. Stamhuis, “PIVlab – Towards User-friendly, Affordable and Accurate Digital Particle Image Velocimetry in MATLAB,” *J. Open Res. Softw.*, vol. 2, no. 1, Oct. 2014, doi: 10.5334/jors.bl.
- [33] B. J. Gemmell, S. P. Colin, J. H. Costello, and J. O. Dabiri, “Suction-based propulsion as a

- basis for efficient animal swimming,” *Nat. Commun.*, vol. 6, no. 1, pp. 1–8, 2015.
- [34] E. G. Drucker and G. V. Lauder, “Experimental hydrodynamics of fish locomotion: Functional insights from wake visualization,” *Integr. Comp. Biol.*, vol. 42, no. 2, pp. 243–257, Apr. 2002, doi: 10.1093/icb/42.2.243.
- [35] Y. Ding and E. Kanso, “Selective particle capture by asynchronously beating cilia,” *Phys. Fluids*, vol. 27, no. 12, p. 121902, Dec. 2015, doi: 10.1063/1.4938558.
- [36] R. C. Darfler and W. W. Tsai, “Method for a low cost hydrokinetic test platform: An open source water flume,” *124th ASEE Annu. Conf. Expo.*, vol. 2017-June, 2017, [Online]. Available: <https://www.scopus.com/inward/record.uri?eid=2-s2.0-85030572432&partnerID=40&md5=9f160bb56019139edba39049d43524f1>.
- [37] R. Waggett and J. H. Costello, “Capture mechanisms used by the lobate ctenophore, *Mnemiopsis leidyi*, preying on the copepod *Acartia tonsa*,” *J. Plankton Res.*, vol. 21, no. 11, pp. 2037–2052, 1999, doi: 10.1093/plankt/21.11.2037.
- [38] N. W. Xu and J. O. Dabiri, “Low-power microelectronics embedded in live jellyfish enhance propulsion,” *Sci. Adv.*, vol. 6, no. 5, p. eaaz3194, Jan. 2020, doi: 10.1126/sciadv.aaz3194.
- [39] T. L. Hedrick, “Software techniques for two- and three-dimensional kinematic measurements of biological and biomimetic systems,” *Bioinspir. Biomim.*, vol. 3, no. 3, p. 034001, Jul. 2008, doi: 10.1088/1748-3182/3/3/034001.
- [40] “DLTdv8 online manual | Hedrick Lab :: Comparative Biomechanics.” https://biomech.web.unc.edu/dltdv8_manual/ (accessed Jun. 10, 2021).

Carlos Abarca

267-897-4026

cqa5253@psu.edu

Current Address:
138 S Atherton Street, Apartment 118
State College, PA 16801

Permanent Address:
3652 Dresher Road
Bensalem, PA 19020

Objective

To pursue a PhD in mechanical or ocean engineering

Education

Pennsylvania State University, University Park, PA
B.S. in Mechanical Engineering

Expected: May 2021
GPA: 3.760

Research/Work Experience

RISE Scholar, Rutgers University, New Brunswick, NJ June 2018-August 2018

- Worked in the Mechanical Engineering department in the lab of Dr. Qingze Zou. Worked on understanding a symbiotic relationship between robots and plants.

CERI Equity REU, Pennsylvania State University, University Park, PA January 2019-April 2019

- Worked in Dr. Margaret Byron's Environmental and Biological Fluid Mechanics lab. Designing tank to keep ctenophores stationary to measure change in fluid motion around their bodies.

Observing the Ocean REU, Texas A&M University, College Station, TX May 2019-August 2019

- Worked as a member of Dr. Robert Hetland's lab in the Oceanography department. Developed method using drone imaging to measure and map out surface flows. Acquired field research experience on multiple cruises. Collected water samples and performed tests in order to find hypoxia.

Millennium Summer Bridge Program Assistant, State College, PA June 2020-August 2020

- Worked with incoming freshmen of the Millennium Scholars Program. Assisted with their summer math class and gave peer mentoring.

Extracurriculars

Society of Hispanic Professional Engineers (SHPE)
American Society of Mechanical Engineers (ASME)
Intramural Sport (soccer, flag football, kickball)

September 2017-May 2021
September 2019-May 2021
September 2017-May 2021

Honors and Awards

Millennium Scholars Program

- A merit-based scholarship program designed to prepare students for the pursuit of doctoral degrees in science, technology, engineering and mathematics (STEM) disciplines.

National Hispanic Scholar

Center for Engineering Outreach and Inclusion Emerging Researcher Award